Conditional success of adaptive therapy: the role of treatment-pausing thresholds revealed by mathematical modeling

Lanfei Sun[1,#], Haifeng Zhang[2,#], Kai Kang[1], Xiaoxin Wang[1], Leyi Zhang[1], Yanan Cai[3,†], Changjing Zhuge[1,*], and Lei Zhang[4,*]

[1]School of Mathematics Statistics and Mechanics, Beijing University of Technology, Beijing 100124, China
[2]School of Mathematical Sciences, Jiangsu University, Zhenjiang, 212013, China
[4]Department of Liver Surgery, Peking Union Medical College Hospital, Chinese Academy of Medical Sciences and Peking Union Medical College, Beijing 100730, China
[3]College of Science and Engineering, James Cook University, Queensland, 4814, Australia
[#]These authors contributed equally
[†]This work was done when Yanan Cai visits Western Sydney University
[*]Correspondence: zhuge@bjut.edu.cn (Changjing Zhuge); zhanglei44@pumch.cn (Lei Zhang)

SUMMARY

Adaptive therapy (AT) improves cancer treatment by controlling the competition between sensitive and resistant cells via treatment holidays. This study highlights the critical role of treatment-pausing thresholds in AT for tumors composed of drug-sensitive and resistant cells. Using a Lotka-Volterra model, the research compares AT with maximum tolerated dose therapy and intermittent therapy, showing that AT's success largely depends on the threshold at which treatment is paused and resumed, as well as the competition between sensitive and resistant cells. Three scenarios of comparison between AT and others are identified: uniform-decline, conditional-improve, and uniform-improve, illustrating that optimizing the treatment-pausing threshold is crucial for AT effectiveness. Tumor composition, including initial tumor burden and the proportion of resistant cells, influences outcomes. Adjusting threshold values enables AT to suppress resistant subclones, preserving sensitive cells, ultimately improving progression-free survival. These findings underscore the importance of personalized strategies for cancer management and enhancing long-term therapeutic outcomes.

KEYWORDS

Adaptive therapy, treatment-holiday threshold, cancer dynamics, mathematical modeling, treatment outcomes

INTRODUCTION

Cancer remains one of the leading causes of death worldwide[1], with its biological complexity and heterogeneity posing significant challenges to conventional therapies such as chemotherapy, radiotherapy, and even immunotherapy[2-4]. Therapeutic resistance, a central obstacle in cancer treatment, arises from the therapeutic selection pressure of pre-existing or induced resistant tumor cells[5-9]. This process drives the evolution of tumor tissue, ultimately leading to the dominance of primary or induced refractory subpopulations, and subsequent relapse and treatment failure[10-12]. The inherent heterogeneity and plasticity of tumor cells often render complete eradication exceedingly difficult, highlighting the necessity of strategies that address the

entire tumor population and its evolutionary dynamics rather than selectively targeting certain subpopulations[4,13,14].

Recently, ecological theory has provided an innovative framework for understanding tumor progression, conceptualizing tumors as ecosystems where drug-sensitive and resistant cells compete for resources[15-23]. Within this ecological framework, cancer cells under drug treatment activate regenerative or protective mechanisms to survive near-lethal stress, enabling them to enter a stem cell-like state and transmit resistance to their progeny[24,25]. This adaptation imposes costs, such as reduced proliferation rates, decreased environmental carrying capacity, and intensified interclonal competition[26,27].

The conventional maximum tolerated dose (MTD) therapy aggressively eliminates sensitive cell populations. However, this strategy inadvertently disrupts competitive equilibria, allowing resistant subclones to proliferate uncontrollably[16,28-31]. This unintended consequence of MTD therapy suggests the limitations of conventional eradication-focused paradigms and highlights the need for therapeutic strategies that preserve sensitive cells to maintain ecological suppression of resistant populations[15,16,32,33].

Adaptive therapy (AT), a dynamic treatment strategy, addresses this challenge by adjusting therapeutic intensity and scheduling in response to real-time tumor burden[16,29,34]. Unlike fixed-dose regimens, AT employs a feedback-controlled approach: treatment is paused when tumor burden declines to certain lower threshold and resumed upon regrowth to an upper threshold. By retaining a reservoir of sensitive cells, this intermittent dosing modality suppresses resistant subclone expansion and prolongs progression-free survival, as evidenced by clinical successes in prostate cancer and other malignancies.

Despite significant advancements[26,31,35-37], further research is needed to refine the optimization of treatment pause thresholds, a core parameter governing AT efficacy, as most existing studies focus on the efficiency of adaptive therapy under predefined thresholds. Several studies have explored the effects of varying thresholds on AT outcomes across different scenarios[36-41], providing valuable insights that underscore the importance of threshold adjustments and establishing a solid foundation for further investigation. However, a deeper understanding of the dynamic mechanisms driving context-dependent outcomes under heterogeneous physiological conditions remains essential. A systematic analysis of how different thresholds will give rise to distinct effects and the underlying dynamical mechanisms, which in turn will enhance conventional empirical threshold selection to achieve an optimal balance between tumor suppression and resistance mitigation. Moreover, it can further facilitate the development of personalized strategies tailored to different conditions. Consequently, quantitative modeling of threshold-driven tumor evolutionary dynamics is essential for advancing precision in adaptive therapy design.

Therefore, this study leverages a mathematical model of tumor evolutionary dynamics to analyze and explain the effects of threshold on the outcomes of AT under various conditions of competitive interactions between sensitive and resistant subpopulations, elucidating the biophysical principles underlying threshold-mediated resistance control. The findings are expected to provide theoretical validation for personalized adaptive therapy protocols, facilitating a paradigm shift toward dynamically optimized cancer management.

In summary, this study, as a state-of-the-art work, systematically investigates the impact of treatment pause thresholds on adaptive therapy outcomes using a Lotka–Volterra model that stimulates the competitive dynamics between drug-sensitive and drug-resistant tumor cell populations. By quantifying the relationship between treatment-pausing threshold and employing time to progression (TTP) as an indicator of PFS, the analysis demonstrates that AT efficacy critically depends on the competition between two subpopulations of cancer cells: while weak competition limits the benefits of AT, strong competition can even allow for the indefinite delay of disease progression. Furthermore, this work also reveals that AT is not uniformly superior to MTD, as

its efficiency depends on tumor composition (initial conditions) and patients' personal conditions (parameters). By comparing the PFS by AT and MTD, it identifies three distinct scenarios, 1) that the which are that AT *uniformly improves* the PFS than MTD regardless of thresholds, 2) that AT has only *conditionally improved* the PFS and 3) that AT has *uniformly worsened* the PFS. These findings highlight the necessity of precise threshold tuning to optimize treatment outcomes. Collectively, these findings provide a theoretical foundation for refining empirical threshold selection and advancing personalized adaptive therapy protocols, thereby paving the way for dynamically optimized cancer management.

RESULTS

Model description

To investigate the effects of different treatment strategies, the tumor dynamics under therapeutic conditions are modelled by the widely used Lotka-Volterra (LV)-type equations[18,36,42–46] because the cancer cells behave more similar to unicellular organism rather than normal human cells[17,47–49]. The cancer cells are further assumed to be classified into two types: drug-sensitive cells (S), which can be killed by drugs, and drug-resistant cells (R), which cannot be eliminated by drugs. These two cell types compete within the cancer microenvironment (Figure 1A), and therefore the LV model is employed as the following ordinary differential equations (ODEs) (1)-(3).

$$\frac{\mathrm{d}S}{\mathrm{d}t} = r_S\left(1-\frac{S+\alpha R}{K}\right)\left(1-\gamma\frac{D(t)}{D_0}\right)S - d_S S, \tag{1}$$

$$\frac{\mathrm{d}R}{\mathrm{d}t} = r_R\left(1-\frac{\beta S+R}{K}\right)R - d_R R, \tag{2}$$

$$N(t) = S(t)+R(t). \tag{3}$$

where $D(t)$ denotes the dose curve of therapeutic agents and S and R represent the burdens of the two types of cells respectively. Equation (1) describes the growth and death of sensitive cells, which means that in the absence of therapy, their proliferation is regulated by intrinsic rate r_S, logistic competition $\left(1-\frac{S+\alpha R}{K}\right)$ and the death rate is d_S. The drug-dependent suppression of sensitive cells is represented by the factor $\left(1-\gamma\frac{D(t)}{D_0}\right)$ where γ is the killing strength of therapeutic agents on sensitive cells. Although this factor is multiplied with the proliferation terms, it is the integrated effective term taking both suppression of proliferation and increasing death rate for simplicity. Equation (2) governs resistant cells, which grow logistically $\left(1-\frac{\beta S+R}{K}\right)$ at rate r_R and die at constant rate d_R, unaffected by the drug. K is the carrying capacity of the cancer microenvironment, indicating the maximum number of cells that can be supported.

Moreover, the model equations (1)–(2) incorporate asymmetric competition between drug-sensitive and drug-resistant cells, characterized by the parameters α and β. Here, α quantifies the inhibitory effect of drug-resistant cells on the growth of sensitive cells, while β represents the impact of drug-sensitive cells on the growth of resistant cells. Specifically, a higher value of α implies that resistant cells more strongly reduce the growth potential of sensitive cells, possibly due to resource competition or indirect suppression via secreted factors (e.g., growth factors, cytokines). Similarly, a higher value of β indicates that sensitive cells exert a stronger influence on the growth of resistant cells, potentially through competition for space, nutrients, or other resources within the tumor microenvironment.

These competitive interactions determine the dominance relationships between the cell populations. For example, in the absence of therapy, coexistence of the two populations is possible under weak competition (i.e., $\alpha < 1$ and $\beta < 1$), whereas strong competition leads to bistability[18,36,50,51]. Specifically, if the resistant cell population is competitively dominant (i.e., $\alpha > 1$ and $\beta < 1$), the sensitive cell population will eventually become extinct; conversely, if $\alpha < 1$ and $\beta > 1$, the resistant cell population will be eliminated[36]. In addition, the competition coefficients also significantly influence treatment outcomes, with a competitive advantage for sensitive cells being crucial for eradicating resistance[52,52-54]. Thus, it is necessary to take these competitive dynamics into account in order to design better strategies.

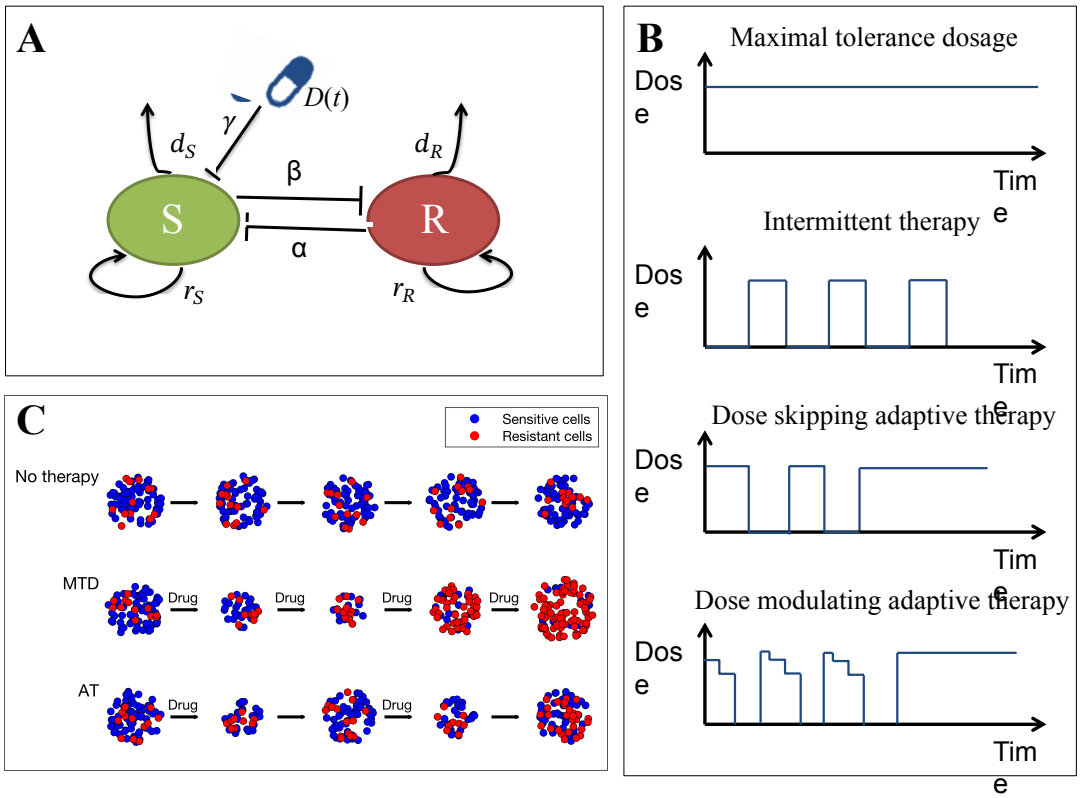

Figure 1: Schematic diagram of cancer dynamics models and illustrations of different treatment strategies and their outcomes. **(A)** A schematic representation of the Lotka-Volterra competition between sensitive cancer cells (S) and resistant cancer cells (R). The interactions between these two cell types are influenced by the carrying capacity K and the competition coefficients α and β. Additionally, in the presence of therapeutic agents, sensitive cells are killed by the drugs. **(B)** Schematic illustration of four typical therapeutic strategies: the maximal tolerance dosage (MTD), intermittent therapy (IT) and dose-skipping adaptive therapy (AT-S), dose-modulating adaptive therapy (AT-M). **(C)** Schematic illustration of tumor burden and compositional evolution under distinct therapeutic strategies.

Different therapeutic strategies are characterized by distinct profiles of the dosing function $D(t)$. Two widely used therapeutic approaches and two regimens of adaptive therapy are considered in this work, including maximum tolerated dose, intermittent therapy (IT), dose-skipping adaptive therapy (AT-S) and dose-modulating adaptive therapy (AT-M) (Figure 1B). The conventional maximum tolerated dose approach seeks to maximize cancer cell eradication by administering the highest dose that a patient can tolerate based on acceptable toxicity levels, which can be defined by continuous administration as (4).

$$\text{(MTD)} \qquad D(t) = D_0, \quad \text{for all} \quad t. \tag{4}$$

As continuous high-intensity dosage leads to the development of therapeutic resistance through Darwinian selection pressures[29], as well as that high dosage of therapeutic agents causes severe toxicity, the therapy holiday, intermittent therapy regimens incorporating treatment holidays were proposed, which strategically suspends drug administration during predefined recovery periods and emerged as a clinically utilized strategy for balancing therapeutic efficacy with toxicity management[43]. The IT strategies can be characterized as deterministic treatment cycles as (5).

$$\text{(IT)} \qquad D(t) = \begin{cases} D_0, & nT \le t \le nT + T_D, \\ 0, & \text{otherwise.} \end{cases} \tag{5}$$

where T is the fixed period of one cycle of treatment, T_D is the duration of drug administration and $n = 1, 2, \cdots$ represents the number of cycles.

As described before, AT dynamically adjusts cancer treatment based on tumor response to prolong efficacy and manage resistance. Two primary approaches within adaptive therapy are dose-skipping and dose-modulating regimens. In dose-skipping adaptive therapy, treatment is administered at the maximum tolerated dose until the tumor burden shrinks to a predetermined threshold (C_{TH0}), for example, 50% of the baseline burden; therapy is then paused, allowing the tumor to regrow to a specific threshold (C_{TH1}), usually, 100% of the baseline, before resuming treatment. In dose-modulating adaptive therapy, treatment doses are adjusted at regular intervals based on tumor response: increasing the dose if the tumor grows and decreasing it if the tumor shrinks. This strategy seeks to tailor therapy dynamically to tumor behavior, potentially reducing toxicity and managing resistance more effectively. Both approaches exploit the competitive dynamics between treatment-sensitive and resistant cancer cells to enhance long-term treatment outcomes and have already succeeded in trials or experiments[29,31,35,55,56]. Based on the above description, the two AT regimens can be formulated as following equations (6) and (7) respectively.

$$\text{(AT-S)} \qquad D(t) = \begin{cases} D_0, & \text{if } N(t) \ge C_{\text{TH0}} N_0 \text{ until } N(t) \ge C_{\text{TH1}} N_0, \\ 0, & \text{if } N(t) \le C_{\text{TH1}} N_0 \text{ and } N'(t) > 0 \text{ until } N(t) \ge C_{\text{TH1}} N_0. \end{cases} \tag{6}$$

$$\text{(AT-M)} \qquad D(t) = \begin{cases} (1+\delta_1) D_0, & \text{if } N(t) \ge C_{\text{TH2}} N_0, \\ D_0, & \text{if } C_{\text{TH1}} N_0 \le N(t) \le C_{\text{TH2}} N_0 \text{ until } N(t) \le C_{\text{TH1}} N_0, \\ (1-\delta_2) D_0, & \text{if } C_{\text{TH0}} N_0 \le N(t) \le C_{\text{TH1}} N_0 \text{ until } N(t) \le C_{\text{TH0}} N_0. \\ 0, & \text{if } N(t) \le C_{\text{TH2}} N_0 \text{ and } N'(t) > 0 \text{ until } N(t) \ge C_{\text{TH2}} N_0. \end{cases} \tag{7}$$

where $N_0 = S_0 + R_0$ is the initial tumor burden and $N'(t)$ is the derivative of $N(t)$ representing whether the tumor burden is growing or shrinking. The threholds satisfies $C_{\text{TH0}} < C_{\text{TH1}} < C_{\text{TH2}}$ and $C_{\text{TH0}} < 1 < C_{\text{TH2}}$. Notably, the dosing strategies (6) and (7) represent state-dependent switching mechanisms rather than closed-form mathematical definitions. This implementation induces history-denpendent therapeutic decision and consequently, the governing equations (1)-(3) constitute delay differential equations with history-dependent terms $D(t)$.

As a state-of-the-art investigation, this study provides comprehensive parametric analysis rather than case-specific parameter estimation. The parameter ranges derive from established experimental and clinical researches[35,36,57-59]. The proliferation rates of sensitive and resistant cells, i.e. r_S and r_R, are derived from *in vitro* experimental data[35], while the drug-induced killing strength γ is sourced from the estimation based on several expriments of cell lines[57]. Given the critical clinical risk associated with large tumor burdens, the initial tumor burden in this study is taken up to 75% of the environmental carrying capacity[58]. The initial proportion of resistant cells follows exsited evolutionary dynamical models[59]. All the baseline parameter values are summarized in Table 1.

Table 1: Model parameters and their ranges.

Parameter	Description	Value or range	Reference
K	Total environmental carrying capacity	10000	
α	Competition coefficient of resistant cells on sensitive cells	$(0, +\infty)$	
β	Competition coefficient of sensitive cells on resistant cells	$(0, +\infty)$	
r_S	Proliferation rate of sensitive cells	0.035	[35]
r_R	Proliferation rate of resistant cells	0.027	[35]
d_S	Death rate of sensitive cells	0.0007	
d_R	Death rate of resistant cells	0.00054	
γ	The killing strength of therapeutic agents	1.5	[57]
D_0	Maximal tolerance dose	1	
$n_0 = \dfrac{N_0}{K}$	Initial tumor burden	$[0, 0.75]$	[58]
$f_R = \dfrac{R_0}{R_0 + S_0}$	Initial proportion of resistant cells	$[0.001, 0.01]$	[59]

The treatment-pausing threshold is crucial for the efficiency of adaptive therapy

To investigate the effect of treatment-pausing thresholds on the outcomes of adaptive therapy, a simplified assumption of neutral competition ($\alpha = \beta = 1$) is considered. The outcomes are primarily characterized by the time to disease progression (TTP), which is typically defined as the time at which the tumor burden grows to a certain percentage greater than its initial burden[35,36,57-59]. For simplicity, this percentage is set to 120% in this study.

As illustrated in the example of tumor evolution under adaptive therapy (Figure 2A), during the initial phase of adaptive therapy, drugs are administered to suppress tumor growth primarily through the depletion of sensitive cells. During this stage, the proportion of sensitive cells is high, which aligns with real-world cases. Following the principles of adaptive therapy, treatment is paused when the tumor burden reaches a predefined treatment-pausing threshold $C_{\mathrm{TH0}}N_0$, conventionally set at 50% of the initial tumor burden, i.e., $C_{\mathrm{TH0}} = 0.5$. The pause allows sensitive cells to repopulate, leading to tumor regrowth. When the tumor burden returns to the initial level N_0, treatment resumes. The treatment-pausing threshold C_{TH0} thus defines a cycle, from the start of treatment to its suspension. These cycles continue until resistant cells dominate the tumor burden, ultimately leading to disease progression.

To further elucidate this phenomenon, phase-plane analysis reveals distinct dynamical regimes with and without treatment (Figure 2B1-B2). In untreated systems, tumor populations evolve toward coexistence equilibria, as indicated by the nullcline, which mathematically corresponds to the diagonal in Figure 2B1. In the presence of treatment (Figure 2B2), the long-term steady state shifts to the upper-left corner, where resistant cells dominate the tumor, and sensitive cells eventually disappear. From a dynamical perspective, treatment exerts selective pressure, pushing the tumor toward a resistant cell-dominant state. Therefore, the significance of treatment pauses lies in allowing the tumor to remain longer in a state dominated by sensitive cells, thereby delaying the transition to resistance. In this regard, increasing the treatment-pausing threshold can slow the transition of tumor composition to a resistant state, which implies it is possible to improve adaptive therapy outcomes by modulating the threshold and preventing continuous treatment from driving the tumor toward resistance via Darwinian selection[16].

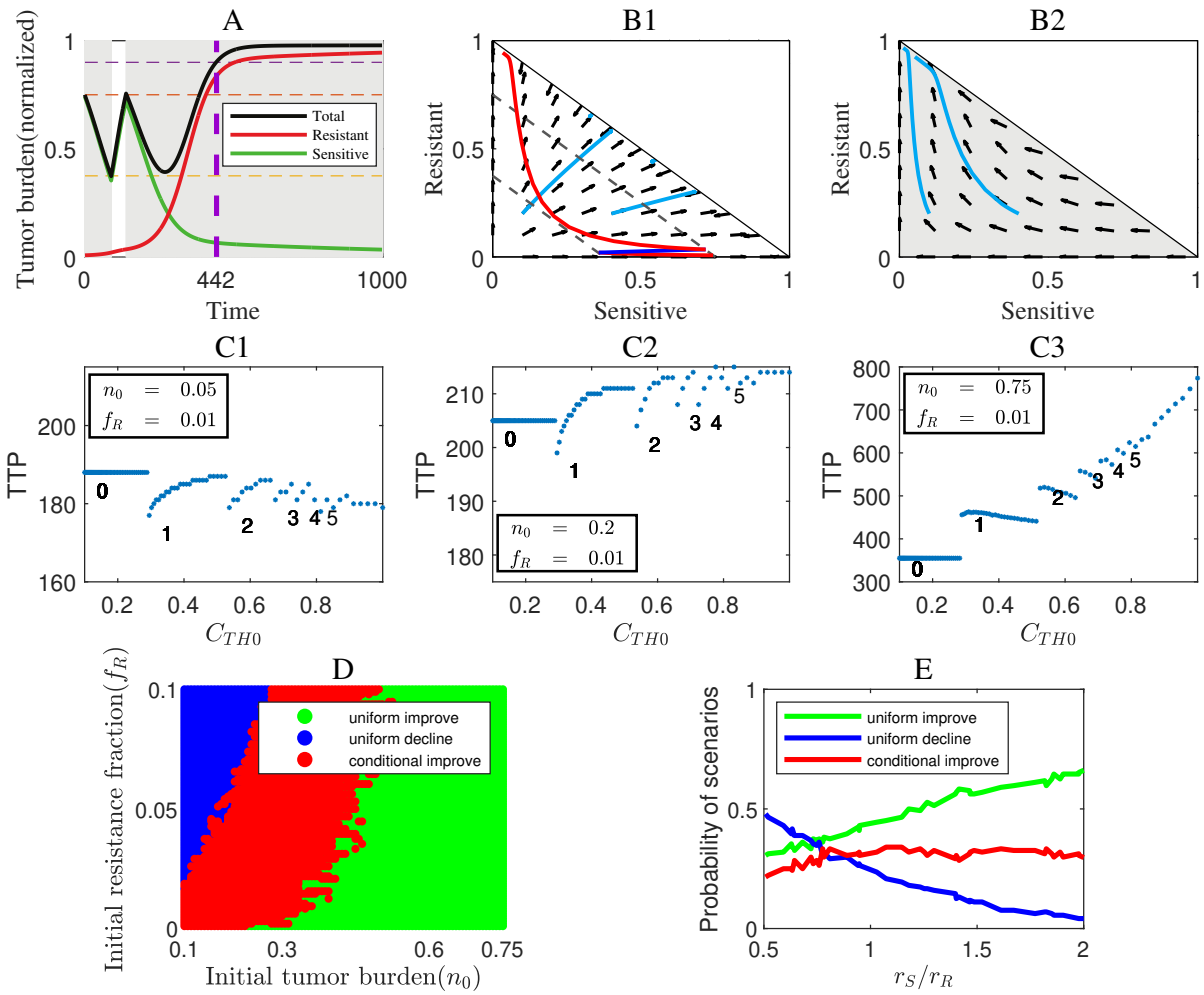

Figure 2: Threshold-mediated therapeutic outcomes under neutral competition ($\alpha = \beta = 1$). **(A)** A representative example of tumor evolution under adaptive therapy (AT), where the initial proportion of resistant cells $f_R = 0.01$ and the initial tumor burden as a fraction of carrying capacity is $n_0 = 0.75$. The purple dashed line represents the time to progression (TTP) under the AT strategy with the threshold $C_{\text{TH0}} = 0.5$; the red, green, and black lines represent resistant cells, sensitive cells, and total tumor burden, respectively. Shaded areas indicate periods of active treatment. **(B1-B2)** The phase diagram and the vector field of tumor evolution with and without treatment. Light blue trajectories illustrate the trajectories with different tumor initial states. The upper right blank region represents situations beyond environmental carrying capacity (K). Panel (B1) illustrates the dynamics without treatment, while panel (B2) shows the cases with maximum tolerated dose strategy. The dark blue trajectory in (B1) shows the dynamics of the total tumor burden without treatment, while the red curve illustrates dynamics under AT as shown in panel (A). **(C1)-(C3)** The impact of changing the treatment-pausing threshold on TTPs under different initial tumor compositions. The numbers on the plots indicate the total number of treatment cycles experienced before disease progression, with 0 cycles of AT corresponding to the MTD strategy. Panel (C1) represents a **uniform-decline** scenario of AT, where the TTPs with AT-S are consistently worse than those with MTD; panel (C2) shows a **conditional-improve** scenario, where AT-S outperforms MTD only for certain threshold values; and panel (C3) demonstrates a **uniform-improve** scenario, where all AT outperforms MTD for all threshold values. **(D)** The dependence of the three scenarios on the initial tumor burden and composition. **(E)** Probability of the three outcome scenarios versus the proliferative fitness ratio r_S/r_R with randomly initial tumor states, demonstrating that a sensitive cell growth advantage ($r_S/r_R > 1$) enhances the AT success probability.

Therefore, the effects of varying the treatment-pausing threshold are examined under different initial tumor states, characterized by the tumor burden (n_0) and the fraction of resistant cells (f_R) (ref. Table 1). As shown in Figures 2C1-C3, altering the treatment-pausing threshold significantly impacted TTP. Notably, when the threshold is too low, meaning the tumor never reached the treatment pause threshold even during the initial cycle, adaptive therapy lacks treatment holidays and effectively becomes equivalent to MTD therapy. Consequently, as C_{TH0} is round 0, TTP of AT is de facto that of MTD therapy, as shown in the leftmost segments of Figures 2C1-C3.

Importantly, for different initial tumor states, three distinct scenarios emerged when comparing adaptive therapy with MTD. The first scenario, *uniform-decline* (Figure 2C1), occurs when adaptive therapy consistently performs worse than MTD, regardless of the threshold. This scenario typically arises in tumors with a low initial tumor burden. The second scenario, *conditionally-improve* (Figure 2C2), occurs when adaptive therapy outperforms MTD only at specific threshold values, suggesting that careful threshold selection is required. The third scenario, *uniform-improve* (Figure 2C3), occurs when adaptive therapy is always superior to MTD.

These findings highlight the complex relationship between the treatment-pausing threshold and TTP. Moreover, as shown in Figures 2C2-C3, the effect of the threshold is neither monotonic nor continuous, exhibiting discontinuities as the number of treatment cycles changes discretely (Figure S1). Specifically, in tumors with a low initial burden (Figures 2C1 and C2), increasing the number of treatment pauses reduces drug exposure, which in turn weakens tumor suppression because under these conditions, the initial tumor burden is low, and therefore, environmental resources remain abundant which makes the changes in the burden of sensitive cells have little impact on the growth rate of resistant cells. In contrast, for tumors with a higher initial burden (Figure 2C3), where environmental resources are constrained, fluctuations in sensitive cell numbers significantly affect the growth of resistant cells. In such cases, increasing the number of treatment pauses enables sensitive cells to grow and exert stronger suppression on resistant cells, leading to a marked increase in TTP. This aligns with clinical observations in prostate cancer, where intermittent dosing preserved therapeutic sensitivity[35].

To further investigate the impact of initial tumor states on these three scenarios, we examined how different initial tumor burdens and initial resistant cell fractions influence adaptive therapy outcomes (Figure 2D). When the initial tumor burden exceeds $0.6K$, adaptive therapy uniformly improves TTP, regardless of the initial proportion of resistant cells. However, when the initial tumor burden is below $0.3K$, adaptive therapy can only conditionally improve TTP, implying that careful selection of the treatment-pausing threshold is crucial. In the worst scenario, when the initial tumor burden is very low and the proportion of resistant cells is relatively high (Figure 2D, top-left), adaptive therapy fails to improve TTP at any threshold, indicating primary resistance. These findings extend prior theoretical work[42] by quantifying phase-transition-like phenomena in threshold-mediated outcomes.

Furthermore, clinical implementation faces inherent uncertainty in tumor state assessment and threshold selection, implying that both the treatment-pausing threshold and the initial tumor burden and resistance fraction exhibit random variability. To address this, Monte Carlo simulations were performed to evaluate the probabilities of the three outcome scenarios under parameter variability (Figure 2E). Inspired by the Norton-Simon Hypothesis[60,61], which posits that sensitive cells typically have a greater fitness advantage than resistant cells (i.e., sensitive cells have a higher intrinsic proliferation rate than resistant cells), we further explored the effect of the relative growth rate of sensitive cells (r_S/r_R) on the probabilities of the three scenarios. By randomly varying the treatment threshold and, while keeping r_S/r_R fixed, randomly altering r_S and r_R, we found that the probability of the *uniform-improve* scenario increases as the relative fitness of sensitive cells increases. When r_S/r_R is small, adaptive therapy is less likely to improve TTP relative to MTD. Conversely, when r_S/r_R is high, indicating that sensitive cells have a significant growth advantage over resistant cells, adaptive therapy is more likely to enhance TTP.

These results confirm that the treatment-pausing threshold has a profound impact on adaptive therapy outcomes and patient-specific tumor characteristics, including initial tumor burden and the relative fitness of sensitive and resistant cells, significantly influence treatment outcomes. These findings align with existing research[26] and demonstrate that r_S/r_R dependence provides quantitative criteria for patient stratification, providing insights for addressing a key challenge in empirical threshold selection[31].

Adaptive therapy is Comparison of the optimal outcomes of four therapeutic strategies

This subsection further compares the efficacy of adaptive therapy and intermittent therapy under the uniform-improve scenario, extending the previous comparison with maximum tolerated dose. As indicated in prior results, the effectiveness of different treatment strategies is influenced by treatment parameters. Therefore, to ensure a fair comparison, treatment parameters must be appropriately aligned. A reasonable approach is to compare strategies based on their best achievable outcomes (Figure 3). Specifically, for intermittent therapy, the optimal treatment cycle and duration should be selected, while for adaptive therapy, the optimal threshold values should be determined.

The optimal parameter combination is determined based on different initial tumor states. Since this study does not focus on identifying these optimal parameters of intermittent therapy, computational details are omitted. However, as previous results suggest that under adaptive therapy in the conditional-improve and uniform-improve scenarios, a threshold closer to 1 generally leads to a longer TTP (Figure 3). In practical applications, a threshold near 1 would necessitate frequent initiation and cessation of treatment, requiring highly precise monitoring of tumor status, which is unrealistic. Similarly, for intermittent therapy, frequent treatment pauses and resumptions are impractical. Given these practical constraints, achieving the true optimal outcome is infeasible. Consequently, only suboptimal treatment outcomes that closely approximate the optimal results are considered as benchmarks for comparison.

For intermittent therapy, the treatment cycle period (T) is examined to range from 7 to 63 time units, with drug administration lasting from 7 to 21 time units (T_D) per cycle. Since this study does not focus on identifying these optimal parameters of IT, computational details are omitted. The result shows that the suboptimal period is $T = 15$ with $T_D = 9$, simulating a regimen in which the patient undergoes both treatment and rest periods within a feasible schedule (Table 1 and equations (5)). For dose-skipping adaptive therapy, the treatment-pausing threshold is set to $C_{\mathrm{TH0}} = 0.98$, while for dose-modulating adaptive therapy, $C_{\mathrm{TH1}} = 1$ and $C_{\mathrm{TH2}} = 1.05$ are selected as the suboptimal treatment parameters (Figure 3A1-A4).

In the uniform-improve scenario for adaptive therapy, a comparison of the suboptimal outcomes across the four treatment strategies (Figure 3A1-A4) reveals that both adaptive therapy strategies result in a longer TTP than intermittent therapy, while intermittent therapy still outperforms MTD. Furthermore, when comparing the two adaptive therapy strategies, AT-M slightly outperforms AT-S. However, considering the operational complexity of AT-M, AT-S is primarily considered in subsequent discussions to balance efficacy with practical feasibility.

From an efficiency perspective, due to factors such as drug side effects, a higher total drug dosage is not necessarily preferable. Therefore, based on the principle of maximizing TTP with the minimum amount of drug, the contribution of unit dosage to TTP is considered a measure of treatment strategy efficiency (equation (8), Figure 3B1-B2):

$$\text{Total dosage} = \int_0^{\mathrm{TTP}} D(t)\,\mathrm{d}t, \quad \text{Efficiency} = \frac{\text{TTP}}{\text{Total dosage}} \tag{8}$$

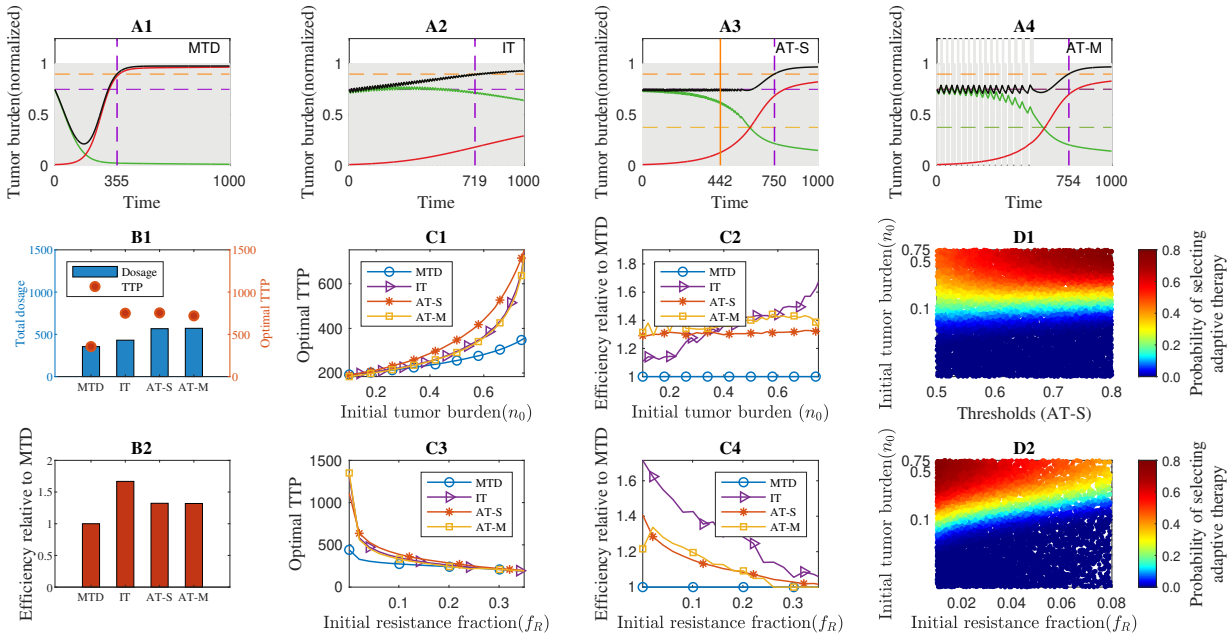

Figure 3: Comparison of optimal outcomes under different therapeutic strategies and success landscapes of adaptive therapy. **(A1)-(A4)** Tumor evolution dynamics under four therapeutic strategies with optimal treatment-pausing thresholds, given $n_0 = 0.75$ and $f_R = 0.01$. The purple dashed line indicates the TTP with optimal treatment parameters, while the orange solid line in (A2) represents the TTP with the conventional 50% threshold ($C_{\mathrm{TH0}} = 0.5$). Red, green, and black curves represent resistant cells, sensitive cells, and total tumor burden, respectively. Shaded regions denote periods of active treatment. For IT, the treatment interval (T) is 15, and the treatment duration (T_D) is 6. For AT-S, the optimal threshold is close to 1, so here C_{TH0} is set to 0.98. Similarly, for AT-M, the middle threshold is $C_{\mathrm{TH1}} = 1$, and the upper threshold is $C_{\mathrm{TH2}} = 1.05$. **(B1)** Cumulative drug toxicity and the corresponding TTP for the four therapeutic strategies. The cumulative toxicity is quantified by the total drug dosage administered before disease progression, given by equation (8). **(B2)** Therapeutic efficiency index, defined as the TTP-to-toxicity ratio as equation (8). Here the efficiency indices are displayed as normalized to that of MTD. **(C1)-(C2)** Effects of varying the initial tumor burden on TTP and the efficiency of the four treatment strategies. **(C3)-(C4)** Effects of varying the initial proportion of resistant cells on TTP and the efficiency of the four treatment strategies. **D1-D2**) Success probability landscapes of AT-S as a function of the initial tumor state and treatment threshold. The color at each point represents the probability of AT-S improving treatment outcomes compared to MTD. (E1) illustrates the dependence of success probability on the initial tumor burden and treatment-pausing threshold with randomly varying f_R, r_S, and r_R, which simulates the uncertainty in tumor proliferation and treatment decisions; while (E2) shows its dependence on the initial fraction of resistant cells and initial tumor burden with randomly varying C_{TH0}, r_S, and r_R.

It is observed that MTD requires the least total drug dosage (Figure 3B1), but this is primarily due to its short TTP. Consequently, MTD's efficiency is the lowest among the four treatment strategies (Figure 3B2). Notably, when efficiency is used as the evaluation criterion, intermittent therapy performs the best (Figure 3B2). This is because intermittent therapy, compared to adaptive therapy, has longer treatment holidays with a relatively smaller decrease in TTP, resulting in a higher contribution of unit drug dosage to TTP (Figure 3B2). This suggests that intermittent therapy is a reasonable option, particularly for patients with lower drug tolerance, which is consistent with clinical practice.

Furthermore, to compare the robustness of the four treatments, the stability of TTP and treatment efficiency under uncertainties in patient physiological conditions and tumor status monitoring is examined. The impact of different initial tumor states on TTP and efficiency under the suboptimal parameters for the four strategies is analyzed (Figure 3C1-C4). For different initial tumor burdens, the trends in TTP for the four treatment strategies under the suboptimal parameters are similar; TTP increases with the tumor burden, which is related to the criteria for determining tumor progression. Since progression is determined based on the initial tumor burden, a larger initial tumor burden necessitates a higher burden for progression to occur, leading to this seemingly counterintuitive result (Figure 3C1). From this perspective, some researchers have proposed a "modifying adaptive therapy" strategy, which delays treatment until the tumor reaches a certain size[62].

Moreover, intermittent therapy shows significant variability with different initial tumor burdens (Figure 3C2). When the tumor burden is small, intermittent therapy is less efficient than adaptive therapy. As the tumor burden increases, this relationship reverses. Therefore, the robustness of intermittent therapy's efficiency is inferior to that of adaptive therapy. This suggests that when adopting intermittent therapy, a more precise assessment of the patient's specific condition is necessary.

On the other hand, both adaptive therapy strategies and intermittent therapy show similar trends in TTP and efficiency with varying initial proportions of resistant cells (Figure 3C3-C4), indicating that the optimal TTP is more influenced by cell composition when the proportion of resistant cells is very low. Notably, when the initial proportion of resistant cells is high, the TTP and efficiency of different treatment strategies are close to those of MTD. This is because, when the initial proportion of resistant cells is high, the determining factor for TTP is no longer the competition between sensitive and resistant cells but rather the proliferation of resistant cells themselves, which reduces the differences between treatment strategies.

Furthermore, similar to the previous results, considering the uncertainty in real-world scenarios, the probability of adaptive therapy being the best strategy is explored under conditions of random tumor growth rates and status monitoring. The probability that adaptive therapy results in a longer TTP than both MTD and intermittent therapy is shown in Figure 3D1-D2. In real scenarios, since the tumor growth rate is unknown and tumor composition is difficult to obtain, the dependence of TTP on treatment-pausing thresholds, initial tumor burden, and initial resistant cell proportion is explored under random variations of other factors. Figure 3D1 shows the dependence of the probability of adaptive therapy outperforming other treatment strategies on different thresholds (C_{CH0} and initial tumor burden (n_0), with the other parameters, including the initial resistant cell proportion (f_R) and the intrinsic growth rates of tumor cells (r_S and r_R) varying randomly. Figure 3D2 shows the dependence of the probability on the intial resistant fraction (f_R) and the initial tumor burden (n_0), with other parameters, C_{TH0}, r_S and r_R, varying randomly.

It can be observed that the probability of selecting adaptive therapy increases significantly when the initial tumor burden is larger. However, when the initial tumor burden is smaller, adaptive therapy does not consistently improve TTP, which aligns with previous findings. Notably, the selection of the treatment-pausing threshold and tumor composition has a weaker impact on the selection of adaptive therapy than the initial tumor burden, indicating that when detailed informa-

tion about tumor components is unavailable, parameters such as the treatment threshold have less influence, with the initial tumor burden playing a key role. On the other hand, TTP is highly sensitive to the selection of the threshold, among other factors (Figures 2 and S2-S6). In other words, the selection of the optimal threshold is also dependent on various tumor states. Therefore, when other parameters are randomly varied, the impact of the threshold on TTP becomes overshadowed by fluctuations in these parameters.

These findings are consistent with clinical observations, emphasizing the importance of a precise understanding of tumor dynamics, particularly intrinsic growth rates. If such tumor information is available, treatment strategy selection can be significantly improved, highlighting the critical importance of accurate tumor characterization, especially regarding tumor dynamics.

Conditional superiority landscapes of adaptive therapy compared to other strategies

The competitive interaction between sensitive (S) and resistant (R) cells, governed by coefficients α and β, fundamentally determines tumor evolution dynamics under therapeutic stress[63-66]. Four distinct regimes emerge based on relative competition strengths: 1) weak competition ($\alpha < 1$, $\beta < 1$), 2) strong competition ($\alpha > 1$, $\beta > 1$), 3) asymmetric competition with $\alpha < 1 < \beta$, or 4) $\beta < 1 < \alpha$. Detailed analyses of $\alpha < 1 < \beta$ and $\beta < 1 < \alpha$ cases demonstrate that therapeutic strategies can induce resistant population extinction under specific conditions[36].

Under strong competition ($\alpha > 1$, $\beta > 1$), untreated tumors evolve toward exclusive dominance of either S or R, depending on initial composition (Figure 4A), mathematically equivalent to equations (1)–(3) possessing two stable steady states. Continuous MTD administration drives the tumor toward a stable steady state where sensitive and resistant cells maintain a fixed ratio with unchanged tumor burden (Figure 4B). In the absence of treatment, the tumor's final state depends on its initial condition, mathematically determined by the basin of attraction in which the system starts. Thus, sensitive cell dominance at initiation leads to resistant cell elimination without treatment, requiring only therapeutic containment to prevent long-term progression. Conversely, initial resistant cell dominance under MTD results in stable tumor burden with constant cellular proportions. The initial tumor burden determines whether disease progression occurs. Even when exceeding progression thresholds, tumor burden stabilizes below carrying capacity. This property renders the "uniformly-improve" scenario inapplicable for strong competition systems, as therapeutic outcomes primarily depend on initial tumor state rather than threshold calibration (Figure 4C). That is, as long as the long-term steady state under treatment remains acceptable (Figure 4B), treatment strategy selection becomes less critical for strong competition cases.

Unlike neutral or strong competition, weak competition ($\alpha < 1$, $\beta < 1$) permits coexistence equilibria regardless of initial states (Figure 5A), while continuous treatment induces resistant dominance through Darwinian selection (Figure 5B). Similar to neutral competition, weak competition exhibits three distinct therapeutic response scenarios (Figure 5C), necessitating strategic treatment selection.

Given clinical uncertainties in weak competition systems, comprehensive parameter-space exploration proves unnecessary and inefficient. The analysis therefore focuses on measurable initial tumor burden (n_0) to evaluate adaptive therapy superiority probability under clinical uncertainty, following previous subsections (Figure 3D1-D2). Less accessible parameters including resistant cell fraction (f_R), thresholds (C_{TH0}), and growth rates (r_S, r_R) are randomized (Figure 5D0-D8). Analysis reveals enhanced adaptive therapy superiority with decreasing α and increasing β (Figure 5D1-D8), consistent with its premise of leveraging sensitive cells to suppress resistant populations. This relationship weakens when resistant cells evade suppression.

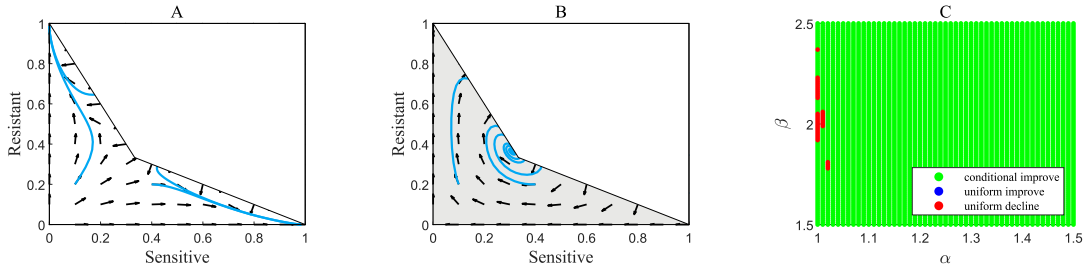

Figure 4: Tumor evolution characteristics under strong competition in the presence of therapy. **(A)** Phase diagram and vector fields of tumor evolution without treatment. The blue lines indicate that the long-term tumor state depends on the initial conditions. The blank region indicates that the effective tumor burden exceeds the carrying capacity ($S + \alpha R > K$ or $\beta S + R > K$). **(B)** Phase diagram and vector fields of tumor evolution with treatment. The long-term tumor dynamics converge to a state characterized by a heterogeneous composition of sensitive and resistant cells. The other features are similar to those in panel (A). **(C)** The dependence of the three scenarios on the competition coefficients α and β, where, in fact, only two scenarios occur: uniform-decline (red) and conditional-improve (green), with the uniform-improve scenario absent. Here the initial tumor burden is taken as $n_0 = 0.75$ and the fraction of resistant cells is taken as $f_R = 0.01$ with the other parameters as shown in Table 1.

Notably, large initial tumor burdens in strong competition systems reduce adaptive therapy selection probability (Figure 5 upper-right quadrant), primarily due to: 1) bistability-mediated tumor burden homeostasis across treatments negating adaptive advantages, and 2) extended progression timelines for large burdens due to progression criteria, diminishing therapeutic differentiation. Surgical intervention may become preferable when tumor burdens approach carrying capacity. Crucially, adaptive therapy selection probability increases with initial tumor burden except at extreme values (Figure 5D0), paralleling neutral competition observations (Figures 2E and 3D1-D2). These findings confirm tumor burden's primacy as the clinically actionable determinant while suggesting benefits from precise competition-strength measurements.

DISCUSSION

Adaptive therapy crucially leverages competitive dynamics to maintain therapeutic-sensitive cell reservoirs that suppress resistant clones, strategically delaying drug resistance evolution while minimizing tumor progression[16]. By preserving sensitive cells through threshold-modulated treatment holidays, adaptive therapy sustains ecological suppression of resistant populations—an advantage over traditional maximum tolerated dose regimens, which inadvertently accelerate resistance[29]. The clinical success of adaptive therapy hinges on its paradigm-shifting principle: harnessing intra-tumor competition to transform therapy-sensitive cells into permanent controllers of resistant cell expansion[33,67]. However, the rule-of-thumb thresholds used in clinical practice may require further research and optimization, as they might not fully account for the complex, dynamic interactions between sensitive and resistant cell populations, and may vary across different tumor types and patient profiles[36-40,68].

This study employs a Lotka-Volterra model to investigate how treatment-pausing thresholds influence adaptive therapy outcomes in tumors composed of drug-sensitive and resistant cells. By simulating tumor dynamics under varying thresholds, initial tumor burdens, and competition coefficients, the analysis identifies three distinct therapeutic scenarios: **uniform-improve** (where AT consistently outperforms MTD regardless of threshold selection), **conditional-improve** (AT efficacy depends on threshold calibration), and **uniform-decline** (MTD superiority). When con-

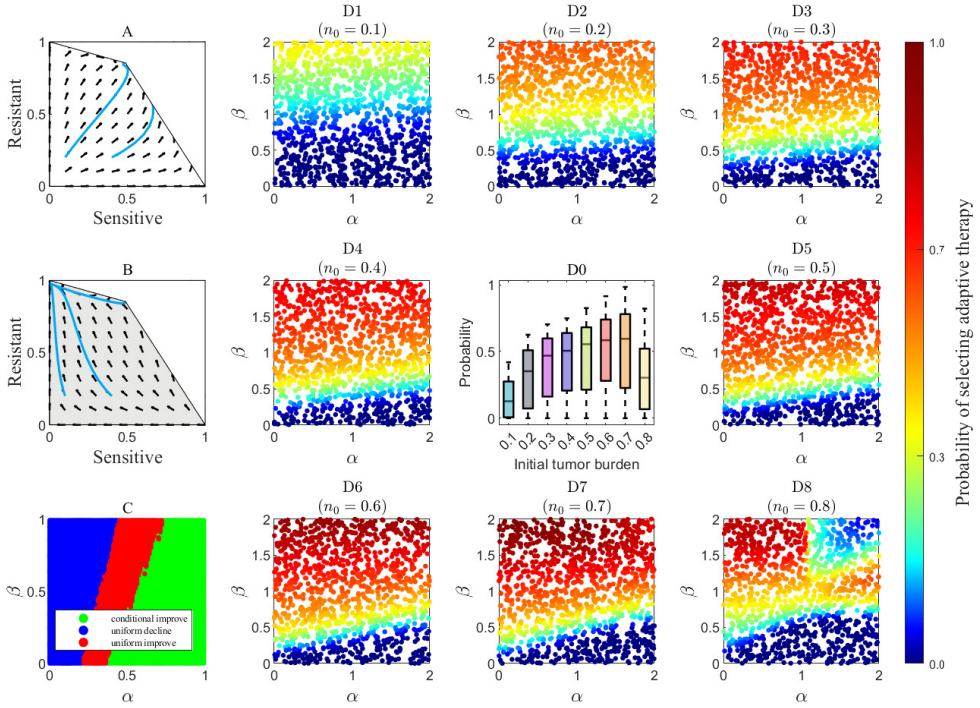

Figure 5: Effectiveness of adaptive therapy under conditions of non-neutral competition. **(A)** Phase diagram and vector field of the dynamics of sensitive and resistant cells in the absence of treatment under weak competition. The blank region represents scenarios where the effective tumor burden exceeds the carrying capacity ($S + \alpha R > K$ or $\beta S + R > K$). The blue lines represent tumor evolution trajectories with different initial tumor states. **(B)** Phase diagram and vector field of the dynamics with treatment. The blue lines show that tumor evolution trajectories all move toward a resistant-dominant state. The other elements in the figure are similar to those in panel (A). **(C)** Dependence of the three scenarios on the competition coefficients, with the initial tumor burden $n_0 = 0.75$, the fraction of resistant cells $f_R = 0.01$, and other parameters set as in Table 1. **(D1-D8)** Dependence of the probability of selecting adaptive therapy on competition coefficients, under different initial tumor burdens. Here, the selection of adaptive therapy refers to the condition where the TTP of adaptive therapy is better than that of other strategies. The fraction of resistant cells f_R, cell division rates r_S and r_R, and treatment-pausing thresholds C_{TH0} are randomly sampled to represent various individual conditions. The sample size is 1200 for each pair of competition coefficient values α and β. **(D0)** Overall dependence of the probability of selecting adaptive therapy on the initial tumor burden. Boxplots show the aggregated probabilities calculated from panels (D1)-(D8). **Note** that panels (D0)-(D8) include both weak and strong competition conditions.

sidering clinical uncertainties in measurement data, generally, the greater the initial tumor burden, the more likely adaptive therapy will outperform other treatment strategies. However, in cases where the tumor burden is excessively high, the advantages of adaptive therapy become irrelevant, and alternative approaches, beyond pharmacological treatment, may be required.

The competitive dynamics between sensitive and resistant cells is also a key factor in tumor evolution under therapeutic stress. In strong competition environments, tumors tend to evolve toward a state dominated by either sensitive or resistant cells, depending on the initial composition. Continuous MTD therapy drives the tumor toward a stable state where the ratio of sensitive to resistant cells remains constant. Thus, the critical factor in treatment outcomes is not the treatment-pausing threshold but rather the impact of the initial tumor state on the final result. In weak competition environments, sensitive and resistant cells can coexist, and adaptive therapy may lead to resistant cell dominance through Darwinian selection. Treatment effectiveness is influenced by the competition coefficients, α and β, with lower α and higher β favoring adaptive therapy. Adaptive therapy prolongs TTP most effectively when sensitive cells maintain a competitive advantage and when initial tumor burden is high, enabling ecological suppression of resistant cells.

This study advances our understanding of adaptive therapy by systematically quantifying the role of treatment-pausing thresholds in modulating tumor evolution under treatment. By integrating ecological competition principles into therapeutic design, the current work provides a mechanistic basis for optimizing intermittent dosing strategies. The findings highlight that adaptive therapy is not universally superior to MTD; its success depends critically on tumor initial state and the treatment-pausing threshold selection. These insights bridge theoretical ecology and clinical oncology, emphasizing the need for dynamic, patient-specific treatment protocols rather than static dosing regimens.

The primary contribution of this work lies in establishing a quantitative relationship between treatment-pausing thresholds and progression-free survival. By categorizing outcomes into three distinct scenarios, the model offers clinicians a potential framework to stratify patients based on measurable parameters such as initial tumor burden and resistant cell fraction. Furthermore, the demonstration that strong competition can stabilize tumor burden indefinitely under specific thresholds has profound implications for managing advanced cancers. These results extend prior work[16,36,39,42] by incorporating threshold-driven mechanism in adaptive therapy.

Limitations of the study

Despite these advances, the study has limitations. First, the binary classification of tumor cells overlooks phenotypic plasticity and continuous heterogeneity, which are critical drivers of therapeutic resistance[13,14,69]. Second, model parameters such as competition coefficients (α, β) are derived from population-level assumptions rather than molecular data, limiting their biological interpretability[70,71]. Third, the Lotka-Volterra framework assumes strict bistability in competitive interactions, neglecting intermediate scenarios where partial resistance or microenvironmental constraints alter dynamics[72-74]. Future studies should integrate single-cell omics to parameterize competition coefficients mechanistically and explore hybrid models combining continuum and spatial interactions. Clinical validation through adaptive therapy trials incorporating real-time biomarker monitoring will be essential to translate these insights into practice.

RESOURCE AVAILABILITY

Lead contact

Requests for further information and resources should be directed to and will be fulfilled by the lead contact, Changjing Zhuge (zhuge@bjut.edu.cn).

Materials availability

This study did not generate new materials.

Data and code availability

- This study did not use any real-world data; all data were generated through computational simulations.
- All original code has been deposited on GitHub (`https://github.com/zhuge-c/AT-0`).
- Any additional information required to reanalyze the data reported in this paper is available from the lead contact upon request.

ACKNOWLEDGMENTS

This work was funded by The National Natural Science Foundation of China (NSFC) via grant 11801020.

AUTHOR CONTRIBUTIONS

Conceptualization: Changjing Zhuge, Lei Zhang; methodology: Changjing Zhuge, Haifeng Zhang; investigation, Lanfei Sun, Changjing Zhuge, Kai Kang, Xiao Wang, Haifeng Zhang; writing-–original draft: Lanfei Sun, Changjing Zhuge, Lei Zhang, Haifeng Zhang; writing-–review & editing: Leyi Zhang, Xiaoxin Wang, Kai Kang, Yanan Cai, Haifeng Zhang, Lei Zhang and Changjing Zhuge; supervision: Changjing Zhuge

DECLARATION OF INTERESTS

The authors declare no competing interests.

SUPPLEMENTAL INFORMATION INDEX

Figure S1: The discontinuous changes in Time to Progression (TTP) under neutral competition conditions as a result of threshold variations. The number of treatment pauses has been altered.

Figures S2-S6: The dependence of TTP on various parameters under neutral competition conditions.

Figures S7-S9: Examples comparing four distinct treatment strategies across three different scenarios under weak competition conditions, along with an analysis of TTP and efficiency index for these examples.

Figure S10: An example of tumor evolution dynamics under strong competition conditions, comparing AT and MTD treatments.

References

1. Bray, F., Laversanne, M., Sung, H., Ferlay, J., Siegel, R.L., Soerjomataram, I., and Jemal, A. (2024). Global cancer statistics 2022: GLOBOCAN estimates of incidence and mortality worldwide for 36 cancers in 185 countries. CA: A Cancer Journal for Clinicians *74*, 229–263. URL: https://acsjournals.onlinelibrary.wiley.com/doi/10.3322/caac.21834. doi: 10.3322/caac.21834.

2. Sung, H., Ferlay, J., Siegel, R.L., Laversanne, M., Soerjomataram, I., Jemal, A., and Bray, F. (2021). Global Cancer Statistics 2020: GLOBOCAN Estimates of Incidence and Mortality Worldwide for 36 Cancers in 185 Countries. CA: A Cancer Journal for Clinicians *71*, 209–249. URL: https://acsjournals.onlinelibrary.wiley.com/doi/10.3322/caac.21660. doi: 10.3322/caac.21660.

3. Marusyk, A., Almendro, V., and Polyak, K. (2012). Intra-tumour heterogeneity: a looking glass for cancer? Nature Reviews Cancer *12*, 323–334. URL: https://www.nature.com/articles/nrc3261. doi: 10.1038/nrc3261.

4. Meacham, C.E., and Morrison, S.J. (2013). Tumour heterogeneity and cancer cell plasticity. Nature *501*, 328–337. URL: https://www.nature.com/articles/nature12624. doi: 10.1038/nature12624.

5. Holohan, C., Van Schaeybroeck, S., Longley, D.B., and Johnston, P.G. (2013). Cancer drug resistance: an evolving paradigm. Nature Reviews Cancer *13*, 714–726. URL: http://dx.doi.org/10.1038/nrc3599https://www.nature.com/articles/nrc3599. doi: 10.1038/nrc3599.

6. Sharma, S.V., Lee, D.Y., Li, B., Quinlan, M.P., Takahashi, F., Maheswaran, S., McDermott, U., Azizian, N., Zou, L., Fischbach, M.A., Wong, K.K., Brandstetter, K., Wittner, B., Ramaswamy, S., Classon, M., and Settleman, J. (2010). A Chromatin-Mediated Reversible Drug-Tolerant State in Cancer Cell Subpopulations. Cell *141*, 69–80. URL: http://dx.doi.org/10.1016/j.cell.2010.02.027. doi: 10.1016/j.cell.2010.02.027.

7. Shi, Z.D., Pang, K., Wu, Z.X., Dong, Y., Hao, L., Qin, J.X., Wang, W., Chen, Z.S., and Han, C.H. (2023). Tumor cell plasticity in targeted therapy-induced resistance: mechanisms and new strategies. Signal Transduction and Targeted Therapy *8*, 113. URL: https://www.nature.com/articles/s41392-023-01383-x. doi: 10.1038/s41392-023-01383-x.

8. Wang, X., Zhang, H., and Chen, X. (2019). Drug resistance and combating drug resistance in cancer. Cancer Drug Resistance *2*, 141–160. URL: https://www.oaepublish.com/articles/cdr.2019.10. doi: 10.20517/cdr.2019.10.

9. Tian, Y., Wang, X., Wu, C., Qiao, J., Jin, H., and Li, H. (2024). A protracted war against cancer drug resistance. Cancer Cell International *24*, 326. URL: https://cancerci.biomedcentral.com/articles/10.1186/s12935-024-03510-2. doi: 10.1186/s12935-024-03510-2.

10. Greaves, M., and Maley, C.C. (2012). Clonal evolution in cancer. Nature *481*, 306–313. URL: https://www.nature.com/articles/nature10762. doi: 10.1038/nature10762.

11. McGranahan, N., and Swanton, C. (2017). Clonal Heterogeneity and Tumor Evolution: Past, Present, and the Future. Cell *168*, 613–628. URL: http://dx.doi.org/10.1016/j.cell.2017.01.018. doi: 10.1016/j.cell.2017.01.018.

12. Turajlic, S., Sottoriva, A., Graham, T., and Swanton, C. (2019). Resolving genetic heterogeneity in cancer. Nature Reviews Genetics *20*, 404–416. URL: http://dx.doi.org/10.1038/s41576-019-0114-6http://www.nature.com/articles/s41576-019-0114-6. doi: 10.1038/s41576-019-0114-6.

13. Gupta, P.B., Fillmore, C.M., Jiang, G., Shapira, S.D., Tao, K., Kuperwasser, C., and Lander, E.S. (2011). Stochastic State Transitions Give Rise to Phenotypic Equilibrium in Populations of Cancer Cells. Cell *146*, 633–644. URL: http://dx.doi.org/10.1016/j.cell.2011.07.026https://linkinghub.elsevier.com/retrieve/pii/S0092867411008245. doi: 10.1016/j.cell.2011.07.026.

14. Marusyk, A., Janiszewska, M., and Polyak, K. (2020). Intratumor Heterogeneity: The Rosetta Stone of Therapy Resistance. Cancer Cell *37*, 471–484. URL: https://doi.org/10.1016/j.ccell.2020.03.007https://linkinghub.elsevier.com/retrieve/pii/S1535610820301471. doi: 10.1016/j.ccell.2020.03.007.

15. Gatenby, R.A. (2009). A change of strategy in the war on cancer. Nature *459*, 508–509. URL: https://www.nature.com/articles/459508a. doi: 10.1038/459508a.

16. Gatenby, R.A., Silva, A.S., Gillies, R.J., and Frieden, B.R. (2009). Adaptive therapy. Cancer Research *69*, 4894–4903. URL: https://aacrjournals.org/cancerres/article/69/11/4894/549572/Adaptive-Therapy. doi: 10.1158/0008-5472.CAN-08-3658.

17. Brown, J.S., Amend, S.R., Austin, R.H., Gatenby, R.A., Hammarlund, E.U., and Pienta, K.J. (2023). Updating the Definition of Cancer. Molecular Cancer Research *21*, 1142–1147. URL: https://aacrjournals.org/mcr/article/21/11/1142/729785/Updating-the-Definition-of-CancerUpdating-the. doi: 10.1158/1541-7786.MCR-23-0411.

18. Aguadé-Gorgorió, G., Anderson, A.R., and Solé, R. (2024). Modeling tumors as complex ecosystems. iScience *27*, 110699. URL: https://linkinghub.elsevier.com/retrieve/pii/S2589004224019242. doi: 10.1016/j.isci.2024.110699.

19. Zahir, N., Sun, R., Gallahan, D., Gatenby, R.A., and Curtis, C. (2020). Characterizing the ecological and evolutionary dynamics of cancer. Nature Genetics *52*, 759–767. URL: http://dx.doi.org/10.1038/s41588-020-0668-4https://www.nature.com/articles/s41588-020-0668-4. doi: 10.1038/s41588-020-0668-4.

20. Bukkuri, A., Pienta, K.J., Hockett, I., Austin, R.H., Hammarlund, E.U., Amend, S.R., and Brown, J.S. (2023). Modeling cancer's ecological and evolutionary dynamics. Medical Oncology *40*, 109. URL: https://doi.org/10.1007/s12032-023-01968-0https://link.springer.com/10.1007/s12032-023-01968-0. doi: 10.1007/s12032-023-01968-0.

21. Bilder, D., Ong, K., Hsi, T.C., Adiga, K., and Kim, J. (2021). Tumour–host interactions through the lens of Drosophila. Nature Reviews Cancer *21*, 687–700. URL: http://dx.doi.org/10.1038/s41568-021-00387-5. doi: 10.1038/s41568-021-00387-5.

22. Hochberg, M.E. (2018). An ecosystem framework for understanding and treating disease. Evolution, Medicine, and Public Health pp. 270–286. doi: 10.1093/emph/eoy032.

23. Brady, R., and Enderling, H. (2019). Mathematical Models of Cancer: When to Predict Novel Therapies, and When Not to. Bulletin of Mathematical Biology *81*, 3722–3731. URL: https://doi.org/10.1007/s11538-019-00640-xhttp://link.springer.com/10.1007/s11538-019-00640-x. doi: 10.1007/s11538-019-00640-x.

24. Attolini, C.S., and Michor, F. (2009). Evolutionary Theory of Cancer. Annals of the New York Academy of Sciences *1168*, 23–51. URL: https://nyaspubs.onlinelibrary.wiley.com/doi/10.1111/j.1749-6632.2009.04880.x. doi: 10.1111/j.1749-6632.2009.04880.x.

25. Vasan, N., Baselga, J., and Hyman, D.M. (2019). A view on drug resistance in cancer. Nature *575*, 299–309. URL: http://dx.doi.org/10.1038/s41586-019-1730-1https://www.nature.com/articles/s41586-019-1730-1. doi: 10.1038/s41586-019-1730-1.

26. Zhang, J., Cunningham, J., Brown, J., and Gatenby, R. (2022). Evolution-based mathematical models significantly prolong response to abiraterone in metastatic castrate-resistant prostate cancer and identify strategies to further improve outcomes. eLife *11*, 1–105. URL: https://elifesciences.org/articles/76284. doi: 10.7554/eLife.76284.

27. Pressley, M., Salvioli, M., Lewis, D.B., Richards, C.L., Brown, J.S., and Staňková, K. (2021). Evolutionary Dynamics of Treatment-Induced Resistance in Cancer Informs Understanding of Rapid Evolution in Natural Systems. Frontiers in Ecology and Evolution *9*, 1–22. URL: https://www.frontiersin.org/articles/10.3389/fevo.2021.681121/full. doi: 10.3389/fevo.2021.681121.

28. Maley, C.C., Aktipis, A., Graham, T.A., Sottoriva, A., Boddy, A.M., Janiszewska, M., Silva, A.S., Gerlinger, M., Yuan, Y., Pienta, K.J., Anderson, K.S., Gatenby, R., Swanton, C., Posada, D., Wu, C.I., Schiffman, J.D., Hwang, E.S., Polyak, K., Anderson, A.R.A., Brown, J.S., Greaves, M., and Shibata, D. (2017). Classifying the evolutionary and ecological features of neoplasms. Nature Reviews Cancer *17*, 605–619. URL: http://dx.doi.org/10.1038/nrc.2017.69https://www.nature.com/articles/nrc.2017.69. doi: 10.1038/nrc.2017.69.

29. Enriquez-Navas, P.M., Kam, Y., Das, T., Hassan, S., Silva, A., Foroutan, P., Ruiz, E., Martinez, G., Minton, S., Gillies, R.J., and Gatenby, R.A. (2016). Exploiting evolutionary principles to prolong tumor control in preclinical models of breast cancer. Science Translational Medicine *8*. URL: https://www.science.org/doi/10.1126/scitranslmed.aad7842. doi: 10.1126/scitranslmed.aad7842.

30. Aktipis, C.A., Boddy, A.M., Jansen, G., Hibner, U., Hochberg, M.E., Maley, C.C., Wilkinson, G.S., Athena Aktipis, C., Boddy, A.M., Jansen, G., Hibner, U., Hochberg, M.E., Maley, C.C., and Wilkinson, G.S. (2015). Cancer across the tree of life: cooperation and cheating in multicellularity. Philosophical Transactions of the Royal Society B: Biological Sciences *370*, 20140219. URL: https://royalsocietypublishing.org/doi/10.1098/rstb.2014.0219. doi: 10.1098/rstb.2014.0219.

31. West, J., Adler, F., Gallaher, J., Strobl, M., Brady-Nicholls, R., Brown, J., Roberson-Tessi, M., Kim, E., Noble, R., Viossat, Y., Basanta, D., and Anderson, A.R. (2023). A survey of open questions in adaptive therapy: Bridging mathematics and clinical translation. eLife *12*, 1–25. URL: https://elifesciences.org/articles/84263. doi: 10.7554/eLife.84263.

32. Gallaher, J.A., Enriquez-Navas, P.M., Luddy, K.A., Gatenby, R.A., and Anderson, A.R. (2018). Spatial heterogeneity and evolutionary dynamics modulate time to recurrence in continuous and adaptive cancer therapies. Cancer Research *78*, 2127–2139. URL: https://aacrjournals.org/cancerres/article/78/8/2127/633375/Spatial-Heterogeneity-and-Evolutionary-Dynamics. doi: 10.1158/0008-5472.CAN-17-2649.

33. West, J., You, L., Zhang, J., Gatenby, R.A., Brown, J.S., Newton, P.K., and Anderson, A.R. (2020). Towards multidrug adaptive therapy. Cancer Research *80*, 1578–1589. URL: https://aacrjournals.org/cancerres/article/80/7/1578/647731/Towards-Multidrug-Adaptive-TherapyTowards. doi: 10.1158/0008-5472.CAN-19-2669.

34. Enriquez-Navas, P.M., Wojtkowiak, J.W., and Gatenby, R.A. (2015). Application of evolutionary principles to cancer therapy. Cancer Research *75*, 4675–4680. doi: 10.1158/0008-5472.CAN-15-1337.

35. Zhang, J., Cunningham, J.J., Brown, J.S., and Gatenby, R.A. (2017). Integrating evolutionary dynamics into treatment of metastatic castrate-resistant prostate cancer. Nature Communications *8*, 1–9. URL: http://dx.doi.org/10.1038/s41467-017-01968-5. doi: 10.1038/s41467-017-01968-5.

36. McGehee, C., and Mori, Y. (2024). A mathematical framework for comparison of intermittent versus continuous adaptive chemotherapy dosing in cancer. npj Systems Biology and Applications *10*, 140. URL: https://www.biorxiv.org/content/early/2024/02/22/2024.02.19.580916https://www.nature.com/articles/s41540-024-00461-2. doi: 10.1038/s41540-024-00461-2.

37. Strobl, M., Gallaher, J., Robertson-Tessi, M., West, J., and Anderson, A. (2023). Treatment of evolving cancers will require dynamic decision support. Annals of Oncology *34*, 867–884. URL: https://doi.org/10.1016/j.annonc.2023.08.008https://linkinghub.elsevier.com/retrieve/pii/S0923753423008062. doi: 10.1016/j.annonc.2023.08.008.

38. Liu, B., Zhou, H., Tan, L., Siu, K.T.H., and Guan, X.Y. (2024). Exploring treatment options in cancer: tumor treatment strategies. Signal Transduction and Targeted Therapy *9*, 175. URL: http://dx.doi.org/10.1038/s41392-024-01856-7https://www.nature.com/articles/s41392-024-01856-7. doi: 10.1038/s41392-024-01856-7.

39. Wang, M., Scott, J.G., and Vladimirsky, A. (2024). Threshold-awareness in adaptive cancer therapy. PLOS Computational Biology *20*, e1012165. URL: http://dx.doi.org/10.1371/journal.pcbi.1012165https://dx.plos.org/10.1371/journal.pcbi.1012165. doi: 10.1371/journal.pcbi.1012165.

40. Tan, R.Z. (2024). Tumour Growth Mechanisms Determine Effectiveness of Adaptive Therapy in Glandular Tumours. Interdisciplinary Sciences: Computational Life Sciences *16*, 73–90. URL: https://doi.org/10.1007/s12539-023-00586-8https://link.springer.com/10.1007/s12539-023-00586-8. doi: 10.1007/s12539-023-00586-8.

41. Strobl, M.A., Martin, A.L., West, J., Gallaher, J., Robertson-Tessi, M., Gatenby, R., Wenham, R., Maini, P.K., Damaghi, M., and Anderson, A.R. (2024). To modulate or to skip: De-escalating PARP inhibitor maintenance therapy in ovarian cancer using adaptive therapy. Cell Systems *15*, 510–525. URL: https://doi.org/10.1016/j.cels.2024.04.003https://linkinghub.elsevier.com/retrieve/pii/S2405471224001182. doi: 10.1016/j.cels.2024.04.003.

42. Strobl, M.A., West, J., Viossat, Y., Damaghi, M., Robertson-Tessi, M., Brown, J.S., Gatenby, R.A., Maini, P.K., and Anderson, A.R. (2021). Turnover Modulates the Need for a Cost of Resistance in Adaptive Therapy. Cancer Research *81*, 1135–1147. URL: https://aacrjournals.org/cancerres/article/81/4/1135/649183/Turnover-Modulates-the-Need-for-a-Cost-of. doi: 10.1158/0008-5472.CAN-20-0806.

43. Mathur, D., Barnett, E., Scher, H.I., and Xavier, J.B. (2022). Optimizing the future: how mathematical models inform treatment schedules for cancer. Trends in Cancer *8*, 506–516. URL: https://doi.org/10.1016/j.trecan.2022.02.005https://linkinghub.elsevier.com/retrieve/pii/S2405803322000413. doi: 10.1016/j.trecan.2022.02.005.

44. Beckman, R.A., Kareva, I., and Adler, F.R. (2020). How Should Cancer Models Be Constructed? Cancer Control *27*, 1–12. URL: https://journals.sagepub.com/doi/10.1177/1073274820962008. doi: 10.1177/1073274820962008.

45. Gatenby, R.A., and Vincent, T.L. (2003). Application of quantitative models from population biology and evolutionary game theory to tumor therapeutic strategies. Molecular Cancer Therapeutics *2*, 919–927. URL: http://mct.aacrjournals.org/content/2/9/919.

46. Gallagher, K., Strobl, M.A., Park, D.S., Spoendlin, F.C., Gatenby, R.A., Maini, P.K., and Anderson, A.R. (2024). Mathematical Model-Driven Deep Learning Enables Personalized Adaptive Therapy. Cancer Research *84*, 1929–1941. URL: https://aacrjournals.org/cancerres/article/84/11/1929/745515/Mathematical-Model-Driven-Deep-Learning-Enableshttps://www.biorxiv.org/content/early/2023/04/30/2023.04.28.538766. doi: 10.1158/0008-5472.CAN-23-2040.

47. Ermini, L., Taurone, S., Greco, A., and Artico, M. (2023). Cancer progression: a single cell perspective. European review for medical and pharmacological sciences *27*, 5721–5747. doi: 10.26355/eurrev{_}202306{_}32812.

48. Pennisi, E. (2018). Is cancer a breakdown of multicellularity? Science *360*, 1391–1391. URL: https://www.science.org/doi/10.1126/science.360.6396.1391. doi: 10.1126/science.360.6396.1391.

49. Deng, Y., Xia, L., Zhang, J., Deng, S., Wang, M., Wei, S., Li, K., Lai, H., Yang, Y., Bai, Y., Liu, Y., Luo, L., Yang, Z., Chen, Y., Kang, R., Gan, F., Pu, Q., Mei, J., Ma, L., Lin, F., Guo, C., Liao, H., Zhu, Y., Liu, Z., Liu, C., Hu, Y., Yuan, Y., Zha, Z., Yuan, G., Zhang, G., Chen, L., Cheng, Q., Shen, S., and Liu, L. (2024). Multicellular ecotypes shape progression of lung adenocarcinoma from ground-glass opacity toward advanced stages. Cell Reports Medicine pp. 101489. URL: https://doi.org/10.1016/j.xcrm.2024.101489https://linkinghub.elsevier.com/retrieve/pii/S2666379124001356. doi: 10.1016/j.xcrm.2024.101489.

50. Chapman, A., del Ama, L.F., Ferguson, J., Kamarashev, J., Wellbrock, C., and Hurlstone, A. (2014). Heterogeneous tumor subpopulations cooperate to drive invasion. Cell Reports *8*, 688–695. URL: http://dx.doi.org/10.1016/j.celrep.2014.06.045. doi: 10.1016/j.celrep.2014.06.045.

51. Aguadé-Gorgorió, G., and Kéfi, S. (2024). Alternative cliques of coexisting species in complex ecosystems. Journal of Physics: Complexity *5*. doi: 10.1088/2632-072X/ad506a.

52. M A, M., Kim, J.Y., Pan, C.H., and Kim, E. (2022). The impact of the spatial heterogeneity of resistant cells and fibroblasts on treatment response. PLOS Computational Biology *18*, e1009919. URL: http://dx.doi.org/10.1371/journal.pcbi.1009919https://dx.plos.org/10.1371/journal.pcbi.1009919. doi: 10.1371/journal.pcbi.1009919.

53. Robertson-Tessi, M., Desai, B., Miti, T., Kumar, P., Yarlagadda, S., Shah, R., Velde, R.V., Miroshnychenko, D., Basanta, D., Anderson, A., and Marusyk, A. (2024). Abstract B008: Therapy-protective peristromal niches mediate positive ecological interaction between therapy-sensitive and therapy-resistant cells, altering the evolution-

ary dynamics of acquired targeted therapy resistance in lung cancers. Cancer Research *84*, B008–B008. URL: https://aacrjournals.org/cancerres/article/84/22_Supplement/B008/749854/Abstract-B008-Therapy-protective-peristromal. doi: 10.1158/1538-7445.TUMBODY-B008.

54. Emond, R., Griffiths, J.I., Grolmusz, V.K., Nath, A., Chen, J., Medina, E.F., Sousa, R.S., Synold, T., Adler, F.R., and Bild, A.H. (2023). Cell facilitation promotes growth and survival under drug pressure in breast cancer. Nature Communications *14*, 3851. URL: https://www.nature.com/articles/s41467-023-39242-6. doi: 10.1038/s41467-023-39242-6.

55. Smalley, I., Kim, E., Li, J., Spence, P., Wyatt, C.J., Eroglu, Z., Sondak, V.K., Messina, J.L., Babacan, N.A., Maria-Engler, S.S., De Armas, L., Williams, S.L., Gatenby, R.A., Chen, Y.A., Anderson, A.R., and Smalley, K.S. (2019). Leveraging transcriptional dynamics to improve BRAF inhibitor responses in melanoma. EBioMedicine *48*, 178–190. URL: https://doi.org/10.1016/j.ebiom.2019.09.023https://linkinghub.elsevier.com/retrieve/pii/S2352396419306279. doi: 10.1016/j.ebiom.2019.09.023.

56. Seyedi, S., Teo, R., Foster, L., Saha, D., Mina, L., Northfelt, D., Anderson, K.S., Shibata, D., Gatenby, R., Cisneros, L.H., Troan, B., Anderson, A.R.A., and Maley, C.C. (2024). Testing Adaptive Therapy Protocols Using Gemcitabine and Capecitabine in a Preclinical Model of Endocrine-Resistant Breast Cancer. Cancers *16*, 257. URL: https://www.mdpi.com/2072-6694/16/2/257. doi: 10.3390/cancers16020257.

57. West, J.B., Dinh, M.N., Brown, J.S., Zhang, J., Anderson, A.R., and Gatenby, R.A. (2019). Multidrug cancer therapy in metastatic castrate-resistant prostate cancer: An evolution-based strategy. Clinical Cancer Research *25*, 4413–4421. URL: https://aacrjournals.org/clincancerres/article/25/14/4413/81985/Multidrug-Cancer-Therapy-in-Metastatic-Castrate. doi: 10.1158/1078-0432.CCR-19-0006.

58. Sunassee, E.D., Tan, D., Ji, N., Brady, R., Moros, E.G., Caudell, J.J., Yartsev, S., and Enderling, H. (2019). Proliferation saturation index in an adaptive Bayesian approach to predict patient-specific radiotherapy responses. International Journal of Radiation Biology *95*, 1421–1426. URL: https://doi.org/10.1080/09553002.2019.1589013https://www.tandfonline.com/doi/full/10.1080/09553002.2019.1589013. doi: 10.1080/09553002.2019.1589013.

59. Grassberger, C., McClatchy, D., Geng, C., Kamran, S.C., Fintelmann, F., Maruvka, Y.E., Piotrowska, Z., Willers, H., Sequist, L.V., Hata, A.N., and Paganetti, H. (2019). Patient-specific tumor growth trajectories determine persistent and resistant cancer cell populations during treatment with targeted therapies. Cancer Research *79*, 3776–3788. URL: https://aacrjournals.org/cancerres/article/79/14/3776/638191/Patient-Specific-Tumor-Growth-Trajectories. doi: 10.1158/0008-5472.CAN-18-3652.

60. Traina, T.A., and Norton, L. (2011). Norton-Simon Hypothesis. In Encyclopedia of Cancer pp. 2557–2559.. Berlin, Heidelberg: Springer Berlin Heidelberg pp. 2557–2559. URL: http://link.springer.com/10.1007/978-3-642-16483-5_4130. doi: 10.1007/978-3-642-16483-5{_}4130.

61. Simon, R., and Norton, L. (2006). The Norton–Simon hypothesis: designing more effective and less toxic chemotherapeutic regimens. Nature Clinical Practice Oncology *3*, 406–407. URL: https://www.nature.com/articles/ncponc0560. doi: 10.1038/ncponc0560.

62. Hansen, E., and Read, A.F. (2020). Modifying Adaptive Therapy to Enhance Competitive Suppression. Cancers *12*, 3556. URL: https://www.mdpi.com/2072-6694/12/12/3556. doi: 10.3390/cancers12123556.

63. Park, J., and Newton, P.K. (2023). Stochastic competitive release and adaptive chemotherapy. Physical Review E *108*, 034407. URL: https://link.aps.org/doi/10.1103/PhysRevE.108.034407. doi: 10.1103/PhysRevE.108.034407.

64. Gatenby, R., and Brown, J. (2018). The evolution and ecology of resistance in cancer therapy. Cold Spring Harbor Perspectives in Medicine *8*. doi: 10.1101/cshperspect.a033415.

65. Wang, T., and Zou, X. (2024). Dynamic analysis of a drug resistance evolution model with nonlinear immune response. Mathematical Biosciences *374*, 109239. URL: https://doi.org/10.1016/j.mbs.2024.109239https://linkinghub.elsevier.com/retrieve/pii/S0025556424000993. doi: 10.1016/j.mbs.2024.109239.

66. Parker, T.M., Gupta, K., Palma, A.M., Yekelchyk, M., Fisher, P.B., Grossman, S.R., Won, K.J., Madan, E., Moreno, E., and Gogna, R. (2021). Cell competition in intratumoral and tumor microenvironment interactions. The EMBO Journal *40*, 1–15. doi: 10.15252/embj.2020107271.

67. Zhang, Y., Vu, T., Palmer, D.C., Kishton, R.J., Gong, L., Huang, J., Nguyen, T., Chen, Z., Smith, C., Livák, F., Paul, R., Day, C.p., Wu, C., Merlino, G., Aldape, K., Guan, X.y., and Jiang, P. (2022). A T cell resilience model associated with response to immunotherapy in multiple tumor types. Nature Medicine *28*, 1421–1431. URL: https://www.nature.com/articles/s41591-022-01799-y. doi: 10.1038/s41591-022-01799-y.

68. Strobl, M., Martin, A.L., West, J., Gallaher, J., Robertson-Tessi, M., Gatenby, R., Wenham, R., Maini, P., Damaghi, M., and Anderson, A. (2023). Adaptive therapy for ovarian cancer: An integrated approach to PARP inhibitor scheduling. bioRxiv. URL: https://www.biorxiv.org/content/early/2023/03/24/2023.03.22.533721. doi: 10.1101/2023.03.22.533721.

69. Brabletz, T., Kalluri, R., Nieto, M.A., and Weinberg, R.A. (2018). EMT in cancer. Nature Reviews Cancer *18*, 128–134. URL: https://www.nature.com/articles/nrc.2017.118. doi: 10.1038/nrc.2017.118.

70. Uthamacumaran, A., and Zenil, H. (2022). A Review of Mathematical and Computational Methods in Cancer Dynamics. Frontiers in Oncology *12*, 1–26. URL: http://arxiv.org/abs/2201.02055http://dx.doi.org/10.3389/fonc.2022.850731https://www.frontiersin.org/articles/10.3389/fonc.2022.850731/full. doi: 10.3389/fonc.2022.850731.

71. Wang, F.S., and Zhang, C. (2020). What to do next to control the 2019-nCoV epidemic? The Lancet *395*, 391–393. URL: https://doi.org/10.1016/S0140-6736(20)30300-7. doi: 10.1016/s0140-6736(20)30300-7.

72. West, J., Ma, Y., and Newton, P.K. (2018). Capitalizing on competition: An evolutionary model of competitive release in metastatic castration resistant prostate cancer treatment. Journal of Theoretical Biology *455*, 249–260. URL: https://doi.org/10.1016/j.jtbi.2018.07.028http://www.sciencedirect.com/science/article/pii/S0022519318303527https://linkinghub.elsevier.com/retrieve/pii/S0022519318303527. doi: 10.1016/j.jtbi.2018.07.028.

73. Noble, R., Burri, D., Le Sueur, C., Lemant, J., Viossat, Y., Kather, J.N., and Beerenwinkel, N. (2021). Spatial structure governs the mode of tumour evolution. Nature Ecology & Evolution *6*, 207–217. URL: https://www.nature.com/articles/s41559-021-01615-9. doi: 10.1038/s41559-021-01615-9.

74. Lorenzi, T., Chisholm, R.H., and Clairambault, J. (2016). Tracking the evolution of cancer cell populations through the mathematical lens of phenotype-structured equations. Biology Direct *11*, 43. URL: http://dx.doi.org/10.1186/s13062-016-0143-4http://biologydirect.biomedcentral.com/articles/10.1186/s13062-016-0143-4. doi: 10.1186/s13062-016-0143-4.